# Thickness-dependent piezoelectric behaviour and dielectric properties of lanthanum modified $BiFeO_3$ thin films

Glenda Biasotto[1], Francisco Moura[2], Cesar Foschini[1], Elson Longo[1], Jose A. Varela[1], Alexandre Z. Simões[3,*]

[1]*Universidade Estadual Paulista, UNESP - Instituto de Química, Laboratório Interdisciplinar em Cerâmica, P.O. Box 355, 14801-907 Araraquara, São Paulo, Brazil*

[2]*Universidade Federal de Itajubá, UNIFEI - Campus Itabira, Rua São Paulo 377, Bairro Amazonas, P.O. Box 355, 35900-37, Itabira, Minas Gerais, Brazil*

[3]*Universidade Estadual Paulista, UNESP - Faculdade de Engenharia de Campus Itabira, Av. Dr Ariberto Pereira da Cunha 333, Bairro Pedregulho, P.O. Box 355, 12.516-410, Guaratinguetá, São Paulo, Brazil*

Received 11 November 2010; received in revised form 4 March 2011; accepted 19 March 2011

**Abstract**

*$Bi_{0.85}La_{0.15}FeO_3$ (BLFO) thin films were deposited on Pt(111)/Ti/$SiO_2$/Si substrates by the soft chemical method. Films with thicknesses ranging from 140 to 280 nm were grown on platinum coated silicon substrates at 500°C for 2 hours. The X-ray diffraction analysis of BLFO films evidenced a hexagonal structure over the entire thickness range investigated. The grain size of the film changes as the number of the layers increases, indicating thickness dependence. It is found that the piezoelectric response is strongly influenced by the film thickness. It is shown that the properties of $BiFeO_3$ thin films, such as lattice parameter, dielectric permittivity, piezoeletric coefficient etc., are functions of misfit strains.*

***Keywords****: thin films, oxides, chemical syntheses, piezoelectricity*

## I. Introduction

Ferroelectromagnets are the class of materials exhibiting coexistence of magnetic and ferroelectric orderings in a certain range of temperature [1–8]. It is known that relatively few multiferroic materials exist as naturally occurring phases, examples of which include $BiFeO_3$ (BFO) [9], $BiMnO_3$ [10], $TbMnO_3$ [11] and $TbMn_2O_5$ [12]. These materials, therefore, not only can be used in magnetic and ferroelectric devices but also have the potential ability to couple the electric and magnetic polarizations, providing an additional degree of freedom in device design and applications. Consequently, ferroelectromagnetism becomes the subject of intensive investigations because these materials potentially offer a whole range of applications, including the emerging field of spintronics [13], data-storage media [14] and multiple-state memories [8]. These multiferroic materials have simultaneous ferromagnetic, ferroelectric and/or ferroelastic ordering [15]. The ferroelectric mechanism in BFO is controlled by the sterochemical activity of the $Bi^{3+}$ $6s^2$ lone pair, responsible of a charge transfer process from $6s^2$ to formally empty 6p orbitals [16,17] while the weak ferromagnetic property can be associated with the residual moment from the canted $Fe^{3+}$ spin structure [18]. The coupling effect between both magnetic and electric behaviours occurs through lattice distortion of BFO [19] and Khomskii [20] has emphasized the different ways to combine magnetism and ferroelectricity in multiferroics materials.

Recently, large ferroelectric polarizations, exceeding those of prototypical ferroelectrics $BaTiO_3$ and $PbTiO_3$, have been reported in heteroepitaxially constrained $BiFeO_3$ thin films [21–24]. Thus, 200-nm-thick $BiFeO_3$ films, grown on (001)c, (110)c, and (111)c $SrTiO_3$ substrates with $SrRuO_3$ as the bottom electrode [21], have remanent polarizations of 55, 80, and 100 μC/cm$^2$, respectively. A 200-nm-thick $BiFeO_3$ film, grown on Si substrate with $SrTiO_3$ as a template layer [22], possesses a remanent polarization of 45 μC/

* Corresponding author: tel: +55 12 3123 2765
fax: +55 12 3123 2800, e-mail: *alezipo@yahoo.com*

$cm^2$. The piezoelectric constant $d_{33}$ shows a dramatic increase from ~30 pm/V for a 100 nm film to ~120 pm/V for a 400 nm film. Wang *et al.* [23] reported a remanent polarization of 50–60 μC/$cm^2$ in the 200-nm-thick $BiFeO_3$ thin film grown by PLD onto the (100) single crystal $SrTiO_3$ substrate. They summarized that the out of plane lattice parameter and the polarization decrease while the piezoelectric coefficient increases as the film thickness increases. Catalan *et al.* [25] have shown that when bismuth ferrite is epitaxially grown as a thin film onto, for example an $SrTiO_3$ [001] substrate, the resulting morphology is monoclinic, where the symmetry lowering distortion arises from in-plane contraction and out of- plane elongation as a result of lattice mismatch between film and substrate.

In other work, Chu *et al.* [26] have evidenced BFO film with a crystal structure of monoclinic phase, which suggests that the polarization direction is close to <111>. Such behaviour has also been confirmed by piezoforce microscopy measurements. The authors have shown that ferroelectricity exists at a minimum thickness down to 2 nm. Chu *et al.* [26] also probed the role of La substitution on the ferroelectric properties of epitaxial $BiFeO_3$ films on $SrTiO_3$-templated Si. This provides a mechanism to engineer the rhombohedral distortion in the crystal and, thus, control domain structure and switching. With the 10 at.% La substitution, the ($Bi_{0.9}La_{0.1}FeO_3$) film showed well-saturated ferroelectric hysteresis loops with a remanent polarization of 45 μC/$cm^2$, a converse piezoelectric coefficient $d_{33}$ of 45 pm/V, and a dielectric constant of 140. Over this range of La substitution, the coercive field systematically decreases in such a way that a coercive voltage of 1 V can be obtained in a 100 nm thick film. These results show promise for the ultimate implementation of this lead-free multiferroic operating at voltages in the range of 2–3 V [27]. Zeches *et al.* [28] using a combination of epitaxial growth techniques in conjunction with theoretical approaches, have shown the formation of a morphotropic phase boundary through epitaxial constraint in lead-free piezoelectric bismuth ferrite ($BiFeO_3$) films. Electric field-dependent studies show that a tetragonal-like phase can be reversibly converted into a rhombohedral-like phase, accompanied by measurable displacements of the surface, making this new lead-free system of interest for probe-based data storage and actuator applications.

A tetragonal-like crystal structure with *c* axis normal to the substrate surface with a small monoclinic distortion of about 0.5° was observed by four-cycle X-ray diffraction [24]. However, a more recent study made by Eerenstein *et al.* [29] argues that the compressive epitaxial strain does not enhance the magnetization and ferroelectric polarization in $BiFeO_3$ thin film. Soon after, Wang *et al.* [30] immediately report the results of additional experiments on this issue. The magnetization of about ~0.5 μB per unit cell for very thin film, although smaller than that in the original magnetic measurement of Wang *et al.* [30], is still much greater than that reported by Eerenstein *et al.* [29], which also progressively decreases as the film thickness is increased to above 120 nm. They suggest that the effect of epitaxial strain can-not be completely ruled out and some additional possible reasons for obtained results are proposed.

If the capacitor area is comparable to the grain size of ferroelectric thin films or electrodes, the influence of grain size and grain boundary cannot be neglected and ferroelectric films and electrodes are required to be thin. For this reason, it is necessary to investigate the influence of grain size, grain boundary and thickness on the electrical properties. The size effects of thin films are different from that of bulk materials. Size effects of thin films include not only grain size but also film thickness. It is difficult to distinguish the size effects derived from grain size from those derived from film thickness because the grain size of the thin films generally changes with film thickness if films are prepared by chemical solution deposition [31]. Furthermore, it has also been reported that the film thickness dependence of a polycrystalline film is different from that of epitaxially grown films [32]. The effect of stress and the existence of a low dielectric constant interfacial layer between the ferroelectric thin film and the substrate are noted to explain these phenomena [33]. In the present investigation and as a natural extension of previous work, $Bi_{0.85}La_{0.15}FeO_3$ thin films were prepared on Pt(111)/Ti/$SiO_2$/Si substrates by the soft chemical method. Structural and electrical properties of the films, mainly related to strain behaviour were investigated by using various techniques with an aim to explore their technological applications [34,35].

However, there are no evidences in the literature showing the influence of the $Bi_{0.85}La_{0.15}FeO_3$ (BLFO) film (obtained by the polymeric precursor method) thickness on the ferroelectric properties [34]. In this article, we report the dependence of the electrical properties from the thickness of BLFO thin films deposited on Pt(111)/Ti/$SiO_2$/Si substrates by the soft chemical method. The influence of BLFO films thickness on leakage behaviour is also discussed.

## II. Experimental

Lanthanum modified bismuth ferrite thin films were prepared by the soft chemical method, as described elsewhere [36]. The films were spin coated on Pt/Ti/$SiO_2$/Si substrates by a commercial spinner operating at 5000 revolutions/min for 30 s (spin coater KW-4B, Chemat Technology). An excess of 5 wt.% of Bi was added to the solution aiming to minimize the bismuth loss during the thermal treatment. The thin films were

annealed at 500°C for 2 hours in the conventional furnace under static air atmosphere. The film thickness was reached by repeating 6, 8 and 10 times the spin-coating and heating treatment cycles. The thickness of the annealed films was measured using scanning electron microscopy (Topcom SM-300) at the transversal section and back-scattering electrons. We have obtained films with the thicknesses in the range of 140 to 280 nm.

Phase analysis of the films was performed at room temperature by X-ray diffraction (XRD) using a Bragg-Brentano diffractometer (Rigaku-DMax 2500PC) and Cu-Kα radiation. Raman measurements were performed using an ISA T 64000 triple monochromator. An optical microscope with 80× objective was used to focus the 514.5 nm radiation from a Coherent Innova 99 $Ar^+$ laser on the sample. The same microscope was used to collect the back-scattered radiation. The dispersed scattering light was detected by a charge-coupled device (CCD) detection system. Surface roughness (RMS) and average grain size was examined by AFM, using tapping mode technique. Next, a 0.5 mm diameter top Au electrode was sputtered through a shadow mask at room temperature. After deposition of the top electrode, the film was subjected to a post-annealing treatment in a tube furnace, at 300°C with constant heating rate of 1°C/min, in oxygen atmosphere for 1 hour. The aim was to decrease eventually present oxygen vacancies. The leakage current-voltage (I-V) characteristic was determined with a voltage source measuring unit (Radiant Technology 6000 A). Piezoelectric measurements were carried out using a setup based on an atomic force microscope in a Multimode Scanning Probe Microscope with Nanoscope IV controller (Veeco FPP-100). In our experiments, piezoresponse images of the films were acquired in ambient air by applying a small ac voltage with amplitude of 2.5 V (peak to peak) and a frequency of 10 kHz while scanning the film surface. To apply the external voltage we used a standard gold coated $Si_3N_4$ cantilever with a spring constant of 0.09 N/m. The probing tip, with an apex radius of about 20 nm, was in mechanical contact with the uncoated film surface during the measurements. Cantilever vibration was detected using a conventional lock-in technique. All measurements were performed at room temperature.

## III. Results and discussion

It is well known that the properties of films are significantly affected by the orientation of the underlying layer, film thickness and atmosphere flow. It is important to control the thickness of the layer due to its strong influence on the grain size, dielectric and ferroelectric properties. For thinner films interfacial "dead layers" which possess poor dielectric properties could appear at the interface film-substrate influencing on the films performance. These dead layers are originated from oxygen interdiffusion, chemical reaction, or structural defects and can be suppressed when film is thicker than 200 nm. Thus, films with 6, 8 and 10 layers were deposited on platinum coated silicon substrates and the XRD pattern is illustrated in Fig. 1. The films were well crystallized at a processing temperature of 500°C. This temperature was chosen because in previous work we have demonstrated that a pure perovskite phase is formed at 500°C for 2 hours with no second phases detected [37]. The characteristic peak for platinum coated silicon (111) substrates was observed in the range of 38° < 2θ < 44°.

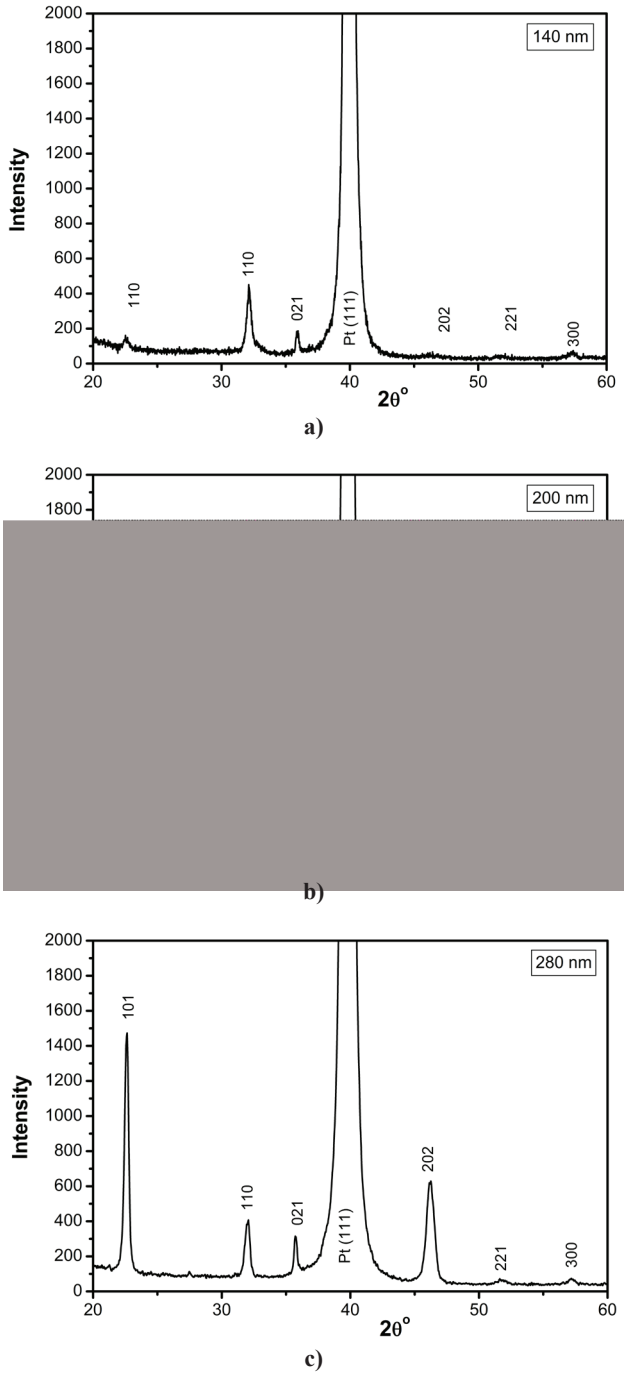


**Figure 1. XRD patterns for BLFO films with different thicknesses: a) 140 nm, b) 200 nm and c) 280 nm**

All films exhibit a polycrystalline structure, except the 280 nm thick films which show (10l)-randomly oriented crystals. Thicker BLFO film consists of randomly oriented perovskite phase. Some orientation-sensitive physical properties, such as dielectric constant, remanent polarization and drive voltage, should vary with the extent of mixed orientations which are different for the films grown with different number of layers. The discussed preferred orientations can be induced by strain due to the differences in lattice parameters and thermal expansion coefficients between BLFO and Pt substrate, indicating that the polar axis is closer to (101) than (110). The diffraction peaks of thicker BLFO films are sharper and stronger than those of thinner BLFO films, indicating better crystallization. XRD results show that the crystalline quality is improved by the increasing thickness of thin films. Although all the films were processed under the same conditions, the thicker films possess better crystallinity because there is a large amount of material deposited on substrate surface influencing the appearance of higher intensities diffraction peaks.

The thickness dependence of the *a* and *c* lattice constants and unit cell volume of the films is shown in Table 1. In this study, we have adopted the Rietveld refinement technique to investigate the crystal structure of the BLFO system. The data were collected from the films annealed at 500°C for 2 hours while clear evidence for the preferred site for lanthanum substitution was obtained. Table 1 illustrates the $R_{wp}$, $R_{exp,}$ and *S* indexes, as well as the lattice parameters (*a* and *c*) and the unit cell volume (*V*). The atomic positions obtained by Rietveld analyses belong to the ICSD card (PDF # 71-2494) with hexagonal symmetry. The quantitative phase analyses for the tetragonal phase were calculated according to the reference of Young *et al.* [38]. BLFO films had a hexagonal structure over the entire thickness range investigated. In addition, the films are polycrystalline without epitaxy along specific orientation. The difference in crystalline properties and inner stress between BLFO films on platinum coated silicon substrates originates from the difference in the lattice mismatch, the thermal expansion coefficient and the crystalline structure. The strain formed is generally released by forming

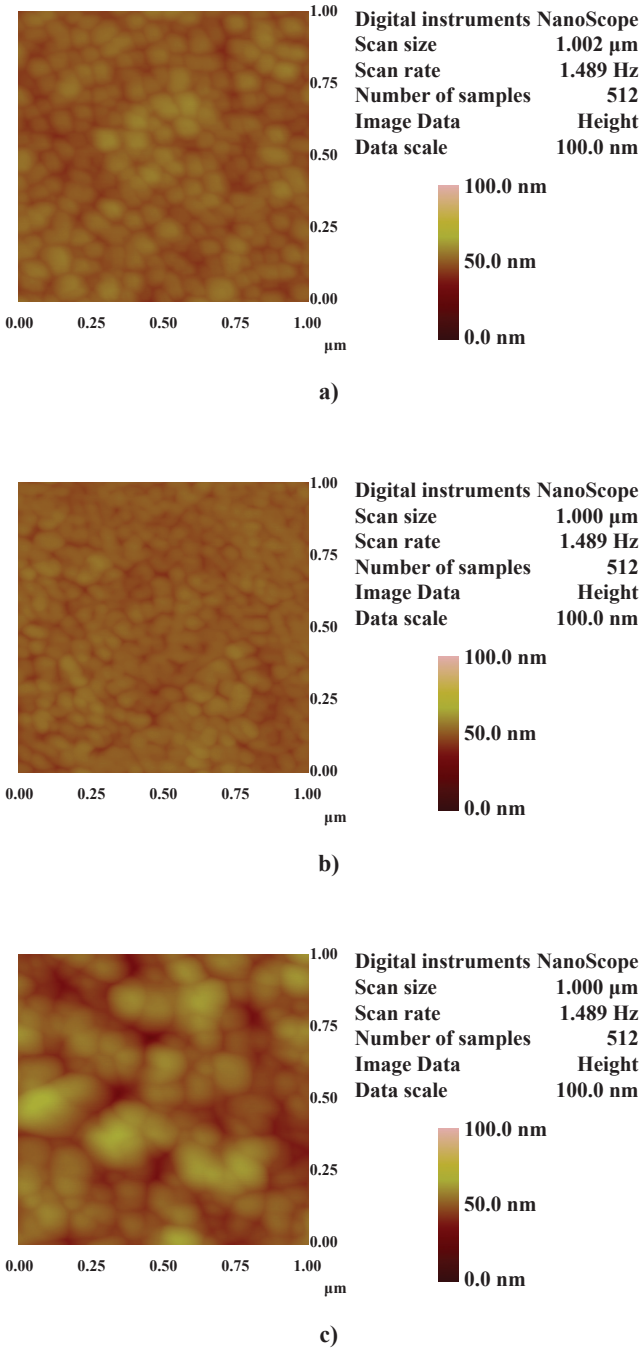


**Figure 2. AFM images of BLFO films with different thicknesses: a) 140 nm, b) 200 nm and c) 280 nm**

**Table 1. Dependence of *a* and *c* lattice constants and unit cell volume for BLFO thin films as a function of thickness**

| | Parameters | 140 (nm) | 200 (nm) | 280 (nm) |
|---|---|---|---|---|
| Refinement indexes | $R_{WP}$ (%) | 10.19 | 10.78 | 12.57 |
| | $R_{EXP}$ | 7.02 | 6.60 | 9.00 |
| | S | 1.44 | 1.62 | 1.39 |
| Lattice parameters | a (Å) | 5.5879 | 5.5942 | 5.6011 |
| | c (Å) | 13.6066 | 13.6386 | 13.6429 |
| | V (Å$^3$) | 367.94 | 369.64 | 371.01 |

disorders at the interface and grain boundaries. This is reasonable since in the thin film form, not only La substitution but also the in-plane stress has effects on the structure [39,40]. The obtained results confirmed that the $Bi^{+3}$ ion was substituted by the $La^{+3}$ ion in the BFO phase and no changes occurred in the refinements. It was observed that $La^{3+}$ substitutes $Bi^{3+}$ only in a perovskite-type unit cell, causing a distorted structure. The covalent interaction, which originates from the strong hybridization between Fe 3*d* and O 2*p* orbitals, plays an important role in the structural distortion of BLFO lattice. Doping with La improves oxygen ion stability in the lattice because some of the Bi ions in the pseudo-perovskite layers containing Fe-O octahedra were substituted by the rare earth ion. From the low *S* values ($S = R_{wp}/R_{exp}$) it can be assumed that the refinement was successfully performed with all the investigated parameters close to literature data [41].

Figure 2 presents the AFM images of the films with different thicknesses. A strongly marked difference in the film microstructure can be observed for different numbers of layers. When the film thickness increased, distinctive plate-like grains were clearly observed. The absence of cracks and fissures indicates that the film has a uniform microstructure. The thinner films present a dense and granular microstructure. The difference in the shape of the grains is related to the amount of material deposited on the substrate surface to crystallize the films. Thinner films possess less material to be crystallized and the grains tend to assume the rounded shape (more energetic). Meanwhile, when the film thickness increased, a large amount of material to be crystallized may lead to elongated grains (a less energetic). The surface roughness was dependent on the film thickness as well as the grain size changing from 53 to 130 nm as the number of layers is increased. Considering that the ferroelectric properties of the BLFO thin films are strongly influenced by the film microstructure, i.e., by the grain size, we expect that, in our case, electrical properties will be sensitive to film thickness. The surface morphology of the BLFO films on $Pt/Ti/SiO_2/Si$ substrates determined by atomic force microscopy (AFM) is shown in Fig. 3. Surface roughness increases with film thickness. The root-mean-square (RMS) roughness of the films is 2.8, 11.0 and 14.0 nm, respectively, for the BLFO films 280, 200 and 140 nm thick. Higher RMS value was observed in thicker films caused by their larger grains.

Raman analysis in the lanthanum modified bismuth ferrite shows the order-disorder degree of the atomic structure at short range (Fig. 3). The modes further split into longitudinal and transverse components due the long electrostatic forces associated with lattice ionicity. Lanthanum atoms substitute bismuth within the perovskite structure having marginal influence in the interactions between the $(Bi_2O_2)^{2+}$ layers and perovskite. The vibrational modes located at 313, 531 and 640 $cm^{-1}$

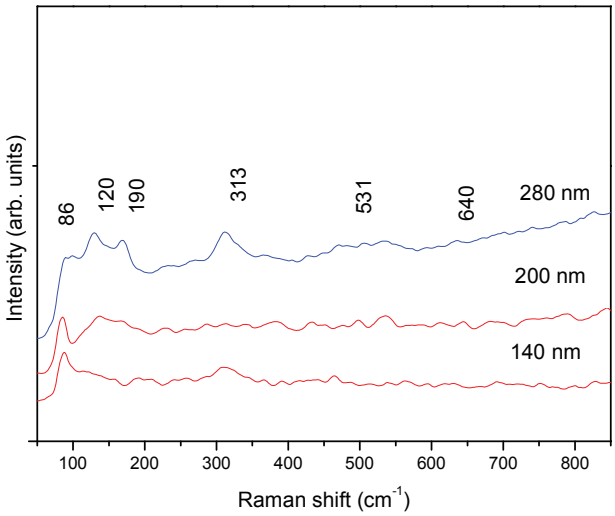


**Figure 3. Micro-Raman spectra for BLFO films with different thicknesses: a) 140 nm, b) 200 nm and c) 280 nm**

result from the $FeO_6$ octahedral (Fe = 5 or Fe = 6). The band located below 200 $cm^{-1}$ is due to the different sites occupied by bismuth within the perovskite layer. As the film becomes thinner, vibrational modes tend to disappear, indicating high structural disordering at short range in the crystal structure as well as the poor crystallinity of the film. A minimum disorder was obtained for the 280 nm thick film while the highest disorder corresponds to a minimum thickness value. The origin of disorder in the BLFO thin films is addressed to the lattice distortion. The suppressed lattice distortion might also cause internal strain in the film as observed in the thicker film. However, near a thickness of 280 nm the lattice distortion is reduced indicating that the driving force for the internal strain was minimized. The reason is that the internal strain changes the microstructure of BLFO films. High internal strains correspond to smaller and coarse grains and, as a result, provide an increase in the number of grain boundaries. Thinner films present large amount of defects associated to the disorder in the BLFO lattice.

The disorder developed in the film is strongly dependent on the thickness showing that the amount of material deposited on the surface of substrate causes a reduction in the defects or disorder of materials. Considering that the ferroelectric properties of BLFO thin films are strongly influenced by film microstructure, i.e., by the grain size, we expect that, in our case, piezoelectric properties will be sensitive to film thickness.

Figure 4 shows the leakage current density as a function of film thickness. The leakage current density at 1.0 V for the 140-nm-thinner film was in the order of $10^{-6}$ $A/cm^2$, but it decreased to the order of $10^{-7}$ $A/cm^2$ for thicker films. The lower leakage current observed for thicker films may be probably attributed to differences in grain size, density and surface structure due to differ-

ences in the number of layers. Since the thinner BLFO films possess higher leakage currents than the thicker ones less resistive films are expected. Two clearly different regions were evident. The current density increases linearly with the external electric field in the region of low electric field strengths, suggesting an ohmic conduction. At higher field the current density increases exponentially, which implies that at least one part of the conductivity results from Schottky or Poole-Frenkel emission mechanisms. The symmetric *J–V* curves were attributed to bulk-limited leakage behaviour rather than interface-limited leakage behaviour in a previous work [42].

The dielectric permittivity and the dissipation factor as a function of film thickness are presented in Fig. 5. The dielectric measurements were carried out at room temperature as a function of frequency in the range from 10 kHz to 1 MHz. The figures show that both dielectric permittivity and the dissipation factor of almost all BLFO films remain fairly constant in this frequency range. The value of $\varepsilon_r$ decreases from 220 to 100 when the film thickness decreases from 280 to 140 nm. This shows that dead layers with lower dielectric constant are formed between the BLFO films and Pt electrodes. Because dead layers and the BLFO films are in series in the capacitance structure, the dielectric permittivity is reduced with decreasing the BLFO film thickness. The *tan δ* changes slightly with increase thickness of the BLFO film. The $\varepsilon_r$ and *tan δ* values are (100, 0.021), (160, 0.017) and (220, 0.024), respectively, for the BLFO films with thickness of 140, 200 and 280 nm. As it can be seen, the dielectric permittivity shows very little dispersion with frequency indicating that the films possess low defect concentrations at the interface film-substrate. The low dispersion of the dielectric permittivity and the absence of any relaxation peak in *tan δ* indicate that an interfacial polarization of the Maxwell Wagner type and an interfacial polarization arisen from the electrode barrier are negligible in the film. The BLFO film had higher relative dielectric permittivity when compared to those previously reported in ceramics or films [43–49]. The observed improvement of dielectric permittivity may be associated with less structural disorder and less two-dimensional stress in the plane of the film.

The piezoelectric behaviour at room temperature is shown in Fig. 6. Butterfly-shaped piezoelectric coefficient versus electric field can be observed for different film thickness. The difference in the piezoelectric behaviour might be attributed to different domain configurations. As usually observed in the relaxor-based "soft" piezoelectric materials, the hysteresis at low fields is attributed to domain motions. In the present work, the hysteresis could also be associated with the domain reorientation, which is prominent for a sample with a multidomain state. Above 30 kV/cm, the hysteresis-free strain is observed, implying a poling state free of domain wall motions induced by the high external electric fields. At 60 kV/cm, the highest electric field in the work, the piezoelectric coefficient is maximum. The thicker film has a higher piezoelectric behaviour in part due to domain reorientation in which a large grain with a multi domain- structure has a higher mobility for polarization reversal than a small grain with a single-domain-structure. Beyond that point, it is possible that a mod-

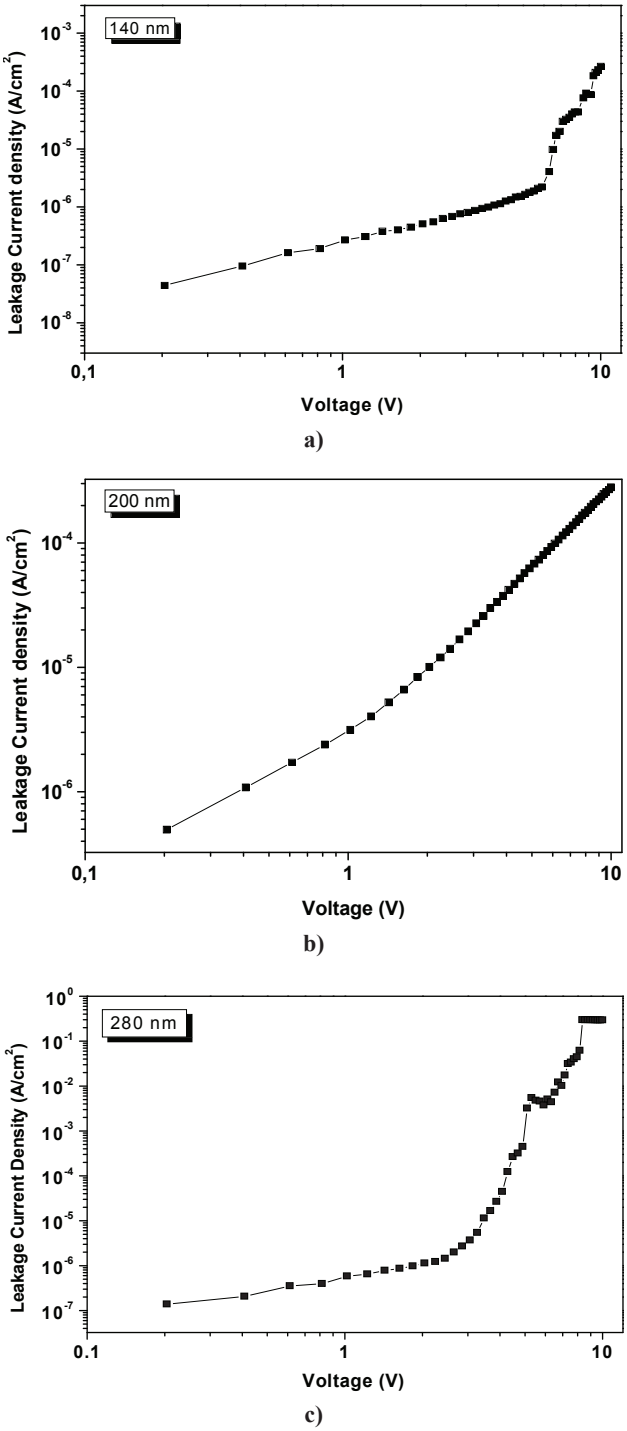


**Figure 4. Leakage current density versus applied electric field for BLFO films with different thicknesses: a) 140 nm, b) 200 nm and c) 280 nm**

est bias field results in the transition from asymmetric to symmetric phase. This field-induced phase transition may be ascribed to the pinching effect, that is, the consequent decrease in free energy difference among polymorphic phases. A careful inspection of the $d_{33}$ - $E$ plots reveals that there are two apparent linear regions at low fields ($E$ < 30 kV/cm) and high fields ($E$ > 70 kV/cm) and one transition region. That corresponds to domains reorientation induced by external electric fields. It is shown that the thicker film exhibited higher piezoelectric strain than the thinner one. The piezoelectric coefficient was 43 pm/V, 40 pm/V and 30 pm/V for the BLFO films with film thickness of 280, 200 and 140 nm, respectively. The improvement of piezoelectric response for the thicker film can be caused by the lower structural disorder and the lower two-dimensional stress in the plane of the film as well as differences in grain size, density and surface structure [50].

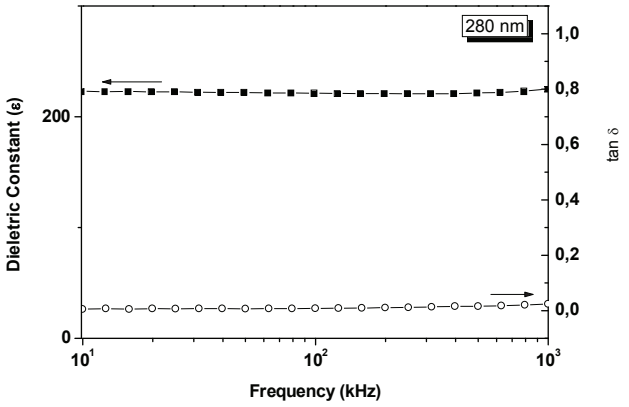


a)

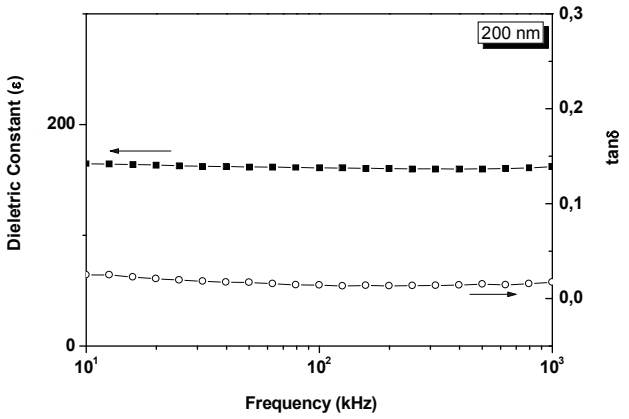


b)

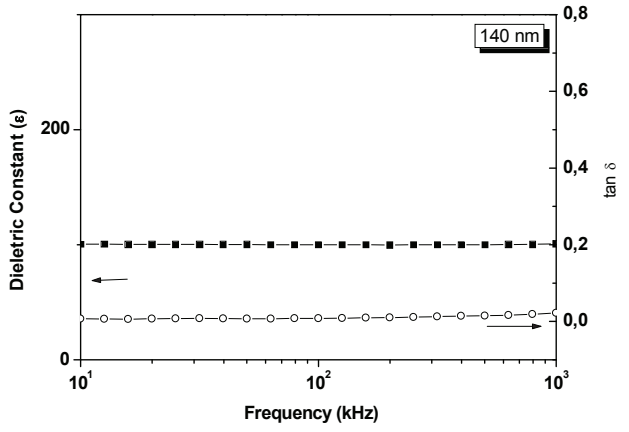


c)

**Figure 5. Dielectric permittivity and dielectric loss spectra of BLFO thin films with different thicknesses: a) 140 nm, b) 200 nm and c) 280 nm**

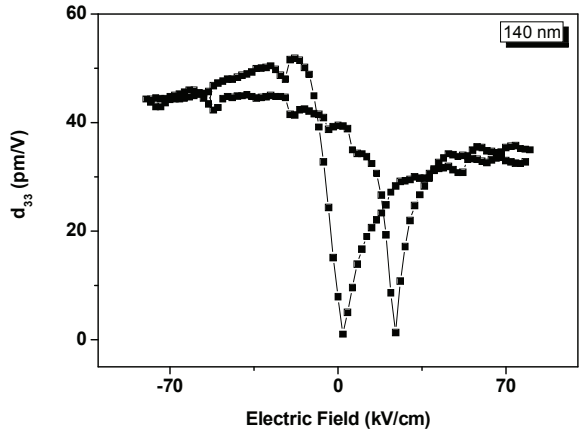


a)

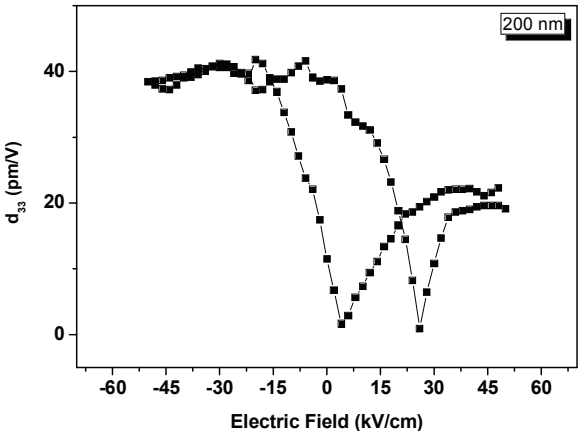


b)

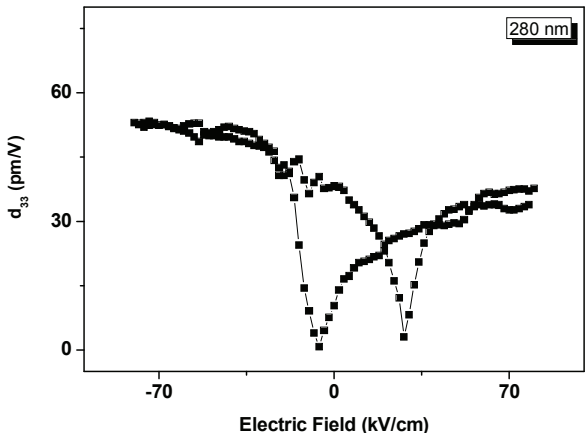


c)

**Figure 6. Piezoelectric coefficient for BLFO films with different thicknesses: a) 140 nm, b) 200 nm and c) 280 nm**

## IV. Conclusions

The thickness effect on piezoelectric properties of $Bi_{0.85}La_{0.15}FeO_3$ (BLFO) thin films fabricated by the soft chemical method was investigated. BLFO films had a hexagonal structure over the entire thickness range investigated. The thinner films possess a dense and granular microstructure, whereas the thicker films have grain aggregation morphology and randomly oriented perovskite phase. The thinner film tends to increase the leakage current as well as decrease the dielectric constant and piezoelectric coefficient due to the internal strain resulting from the electrode/ferroelectric interfacial layer. The optimal film thickness is close to 280 nm. The results of these studies are very promising and suggest that the BLFO thin films can be used as a storage element in nonvolatile ferroelectric random access memories.

**Acknowledgements:** The authors gratefully acknowledge the financial support of the Brazilian financing agencies FAPESP, CNPq and CAPES.

## References

1. N.A. Spaldin, M. Fiebig, "The Renaissance of Magnetoelectric Multiferroics", *Science*, **309** (2005) 391–392.
2. W. Eerenstein, N.D. Mathur, J.F. Scott," Multiferroic and Magnetoelectric Materials", *Nature*, **442** (2006) 759–765.
3. S.W. Chong, N. Mostovoy, "A magnetic twist for ferroelectricity", *Nat. Mater.*, **6** (2007) 13–20.
4. R. Ramesh, N.A. Spaldin, "Multiferroics: progress and prospects in thin films", *Nat. Mater.*, **6** (2007) 21–29.
5. W. Eerenstein, M. Wiora, J.L. Prieto, J.F. Scott, N.D. Mathur, "Giant sharp and persistent converse magnetoelectric effects in multiferroic epitaxial heterostructures", *Nat. Mater.*, **6** (2007) 348–356.
6. M. Fiebig, "Revival of the magnetoelectric effect" *J. Phys. D.*, **38** (2005) R123–R152.
7. G. Catalan, "Magnetocapacitance without magnetoelectric coupling", *Appl. Phys. Lett.*, **88** (2006) 102902–102904.
8. N.A. Hill, "Why are there so few magnetic ferroelectrics?", *J. Phys. Chem. B*., **104** (2000) 6694–6709.
9. A.H.M. Gonzalez, A.Z. Simões, L.S. Cavalcante, E. Longo, J.A. Varela, C.S. Riccardi, "Soft chemical deposition of $BiFeO_3$ multiferroic thin films", *Appl. Phys. Lett.*, **90** (2007) 052906–052908.
10. A.M. dos Santos, S. Parashar, A.R. Raju, Y.S. Zhao, A.K. Cheetham, C.N.R. Rao, "Evidence for the likely occurrence of magnetoferroelectricity in the simple perovskite, $BiMnO_3$", *Solid State Commun.*, **122** (2002) 49–52.
11. T. Kimura, T. Goto, H. Shintani, K. Ishizaka, T. Arima, Y. Tokura, "Magnetoelectric phase diagrams of orthorhombic $RMnO_3$", *Phys. Rev. B.*, **71** (2005) 224425–224236.
12. N. Hur, S. Park, P.A. Sharma, J.S. Ahn, S. Guha, S.W. Cheong, "Electric polarization reversal and memory in a multiferroic material induced by magnetic fields", *Nature*, **429** (2004) 392–395.
13. H. Bea, M. Bibes, M. Sirena, G. Herranz, K. Bouzehouane, E. Jacquet, S. Fusil, P. Paruch, M. Dawber, J.P. Contour, A. Barthelemy, "Tunnel magnetoresistance and robust room temperature exchange bias with multiferroic $BiFeO_3$ epitaxial thin films", *Appl. Phys. Lett.*, **90** (2006) 062502–062504.
14. M. Fiebig, Th. Lottermoser, D. Frhlich, A.V. Golsev, R.V. Pisarev, "Observation of coupled magnetic and electric domains", *Nature*, **419** (2002) 818–820.
15. H. Schmid, "On the birefringence of magnetoelectric $BiFeO_3$", *Ferroelectrics.*, **204** (1994) 23–33.
16. R. Seshadri, N.A. Hill, "Visualizing the role of Bi 6s "lone pairs" in the off-center ferromagnetic $BiMnO_3$", *Chem. Mater.*, **13** (2001) 2892–2899.
17. T. Shishidou, N. Mikamo, Y. Uratani, F. Ishii, T. Oguchi., "First-principles study on the electronic structure of bismuth transition-metal oxides", *J. Phys. Condens. Matter.*, **16** (2004) S5677–S5683.
18. P. Fischer, M. PoIomska, I. Sosnowskag, M. Szymanskig, "Temperature dependence of the crystal and magnetic structures of $BiFeO_3$", *J. Phys. C.: Solid State Phys*., **13** (1980) 1931–1937.
19. S-W. Cheong, M. Mostovoy, "Multiferroics: a magnetic twist for ferroelectricity", *Nat. Mater.*, **6** (2007) 13–20.
20. D.I. Khomskii, "Multiferroics: Different ways to combine magnetism and ferroelectricity", *J. Magn. Magn. Mater.*, **360** (2006) 1–8.
21. J.F. Li, J. Wang, M. Wuttig, R. Ramesh, N. Wang, B. Ruette, A.P. Pyatakov, A.K. Zvezdin, D. Viehland, "Dramatically enhanced polarization in (001), (101), and (111) $BiFeO_3$ thin films due to epitiaxial-induced transitions", *Appl. Phys. Lett.*, **84** (2004) 5261–5263.
22. J. Wang, H. Zheng, Z. Ma, S. Prasertchoung, M. Wuttig, R. Droopad, J. Yu, K. Eisenbeiser, R. Ramesh, "Epitaxial $BiFeO_3$ thin films on Si", *Appl. Phys. Lett.*, **85** (2004) 2574–2576.
23. Y. Lin, A. Boker, Q. Wang, S. Long. K. Sill, A. Balazs, T.P. Russel, "Self-directed self-assembly of nanoparticle/copolymer mixtures", *Science*, **434** (2005) 55–59.
24. F. Bai, J. Wang, M. Wuttig, J.F. Li, N. Wang, A.P. Pyatakov, A.K. Zvezdin, L.E. Cross, D. Viehland, "Destruction of spin cycloid in (111)c-oriented $BiFeO_3$ thin films by epitiaxial constraint: Enhanced polarization and release of latent magnetization", *Appl. Phys. Lett.*, **86** (2005) 032511–032513.
25. G. Catalan, J.F. Scott, "Physics and applications of bismuth ferrite", *Adv. Mater.*, **21** (2009) 2463–2485.
26. Y.H. Chu, T. Zhao, M.P. Cruz, Q. Zhan, P.L. Yang, L.W. Martin, M. Huijben, C.H. Yang, F. Zavaliche, H. Zheng, R. Ramesh, "Ferroelectric size effects in multiferroic $BiFeO_3$ thin films", *Appl. Phys. Lett.*, **90** (2007) 252906–252908.

27. Y.H. Chu, Q. Zhan, C.-H. Yang, M.P. Cruz, L.W. Martin, T. Zhao, P. Yu, R. Ramesh, P.T. Joseph, I.N. Lin, W. Tian, D.G. Schlom, "Low voltage performance of epitaxial $BiFeO_3$ films on Si substrates through lanthanum substitution", *Appl. Phys. Lett.*, **92** (2008) 102909–102911.
28. R.J. Zeches, M.D. Rossell, J.X. Zhang, A.J. Hatt, Q. He, C.-H. Yang, A. Kumar, C.H. Wang, A. Melville, C. Adamo, G. Sheng, Y.-H. Chu, J.F. Ihlefeld, R. Erni, C. Ederer, V. Gopalan, L.Q. Chen, D.G. Schlom, N.A. Spaldin, L.W. Martin, R. Ramesh, "A strain-driven morphotropic phase boundary in $BiFeO_3$", *Science*, **326** (2009) 977–980.
29. W. Eerenstein, F.D. Morrison, J. Dho, M.G. Blamire, J.F. Scott, N.D. Mathur, Comment on "Epitaxial $BiFeO_3$ multiferroic thin film heterostructures", *Science*, **307** (2005) 1203a.
30. J. Wang, A. Scholl, H. Zheng, S.B. Ogale, D. Viehland, D.G. Schlom, N.A. Spaldin, K.M. Rabe, M. Wuttig, L. Mohaddes, J. Neaton, U. Waghmare, T. Zhao, R. Ramesh, Response to Comment on "Epitaxial $BiFeO_3$ multiferroic thin film heterostructures", *Science*, **307** (2005) 1203b.
31. A.Z. Simões, M.A. Ramirez, N.A. Perucci, C.S. Riccardi, E. Longo, J.A. Varela, "Retention characteristics in $Bi_{3.25}La_{0.75}Ti_3O_{12}$ thin films prepared by the polymeric precursor method", *Appl. Phys. Lett.*, **86** (2005) 112909–112911.
32. T. Hayashi, N. Oji, H. Maiwa, "Film thickness dependence of dielectric properties of $BaTiO_3$ thin films prepared by sol-gel method", *Jpn. J. Appl. Phys.*, **33** (1994) 5277–5280.
33. J.F.M. Cillessen, M.W.J. Prins, R.W. Wolf, "Thickness dependence of the switching voltage in all-oxide ferroelectric thin-film capacitors prepared by pulsed laser deposition", *J. Appl. Phys.*, **81** (1997) 2777–2781.
34. A.Z. Simoes, A.H.M. Gonzalez, C.S. Riccardi, E.C. Souza, F. Moura, M.A. Zaghete, E. Longo, J.A. Varela, "Ferroelectric and dielectric properties of lanthanum modified bismuth titanate thin films obtained by the polymeric precursor method", *J. Electroceram.*, **13** (2004) 65–70.
35. A.Z. Simões, B.D. Stojanovic, M.A. Zaghete, C.S. Riccardi, A. Ries, F. Moura, E. Longo, J.A.Varela, "Electrical characterization of lanthanum-modified bismuth titanate thin films obtained by the polymeric precursor method", *Integr. Ferroelectric.*, **60** (2004) 21–31.
36. A.Z. Simões, L.S. Cavalcante, C.S. Riccardi, J.A. Varela, E. Longo, "Ferroelectric and dielectric behaviour of $Bi_{0.92}La_{0.08}FeO_3$ multiferroic thin films prepared by soft chemistry route", *J. Sol-Gel Sci. Technol.*, **3** (2007) 269–273.
37. A.Z. Simões, A.H.M. Gonzalez, L.S. Cavalcante, C.S. Riccardi, E. Longo, J.A. Varela, "Ferroelectric characteristics of $BiFeO_3$ thin films prepared via a simple chemical solution deposition", *J. Appl. Phys.*, **101** (2007) 074108–074113.
38. R.A. Young, A. Sakthivel, T.S. Moss, C.O. Paiva-Santos, "*DBWS*-9411 - an upgrade of the *DBWS**.* programs for Rietveld refinement with PC and mainframe computers", *J. Appl. Cryst.*, **28** (1995) 366–367.
39. J. Wang, J.B. Neaton, H. Zheng, V. Nagarajan, S.B. Ogale, B. Liu, D. Viehland, V. Vaithyanathan, D.G. Schlom, U.V. Waghmare, N.A. Spaldin, K.M. Rabe, M. Wuttig, R. Ramesh, "Epitaxial $BiFeO_3$ multiferroic thin film heterostructures", *Science*, **299** (2003) 1719–1722.
40. J. Li, J. Wang, M. Wuttig, R. Ramesh, N. Wang B. Ruette, A.P. Pyatakov, A.K. Zvezdin, D. Viehland, "Influence of Mn and Nb dopants on electric properties of chemical-solution-deposited $BiFeO_3$ films", *Appl. Phys. Lett.*, **84** (2004) 5261–5263.
41. S. Luo, Y. Noguchia, M. Miyayamab, T. Kudo, "Rietveld analysis and dielectric properties of $Bi_2WO_6$–$Bi_4Ti_3O_{12}$ ferroelectric system", *Mater. Res. Bull.*, **36** (2001) 531–540.
42. Y.H. Lee, J.M. Wu, Y.L. Chueh, L.J. Chou, "Low temperature growth and interface characterization of $BiFeO_3$ thin films with reduced leakage current", *Appl. Phys. Lett.*, **87** (2005) 172901–172903.
43. Z.H. Sun, C.H. Kim, H.B. Moon, Y.H. Jang, J.H. Cho, C.S. Liang, J.M. Wu, M.C. Chang, "Improved dielectric properties of $CaCu_3Ti_4O_{12}$ thin films on oxide bottom electrode of $La_{0.5}Sr_{0.5}CoO_3$", *Thin Solid Films*, **518** (2010) 3417–33421.
44. M. Mahesh Kumar, V.R. Palkar, K. Srinivas, S.V. Suryanarayana, "Ferroelectricity in a pure BiFeO[sub 3] ceramic", *Appl. Phys. Lett.*, **76** (2000) 2764–2766.
45. J.K. Kim, S.S. Kim, W. Kim, "A review on inorganic nanostructure self-assembly", *Mater. Lett.*, **59** (2005) 4006–4008.
46. H. Liu, Z. Liu, Q.Liu, K. Yao, "Ferroelectric properties of $BiFeO_3$ films grown by sol–gel process", *Thin Solid Films*, **500** (2006) 105–109.
47. V.R. Palkar, J. John, R. Pinto, "Observation of saturated polarization and dielectric anomaly in magnetoelectric $BiFeO_3$ thin films", *Appl. Phys. Lett.*, **80** (2002) 1628–1630.
48. A.K. Pradhan, K. Zhang, D. Hunter, J.B. Dadson, G.B. Loutts, P. Bhattacharya, R. Katiyar, J. Zhang, U.N. Roy, Y. Cui, A. Burger, "Magnetic and electrical properties of single-phase multiferroic $BiFeO_3$", *J. Appl. Phys.*, **97** (2005) 093903–093906.
49. G.L. Yuan, S.W. Or, Y.P. Wang, Z.G. Liu, J.M. Liu, "Preparation and multi-properties of insulated single-phase $BiFeO_3$ ceramics", *Solid State Commun.*, **138** (2006) 76–81.
50. A.Z. Simões, C.S. Riccardi, L.S. Cavalcante, J.A. Varela, E. Longo, "Size effects of polycrystalline lanthanum modified $Bi_4Ti_3O_{12}$ thin films", *Mater. Res. Bull.*, **43** (2008) 158–167.